Journal of Alloys and Compounds 503 (2010) 445–448

Contents lists available at ScienceDirect

Journal of Alloys and Compounds

journal homepage: www.elsevier.com/locate/jallcom

Synthesis of $LiVO_3$ thin films by spray pyrolysis technique

A. Bouzidi [a,*], N. Benramdane [a], M. Medles [a], M. Khadraoui [a], S. Bresson [b], C. Mathieu [c], R. Desfeux [c], M. El. Marssi [d]

[a] Laboratoire d'Elaboration et de Caractérisations des Matériaux, Département d'Électronique, Université Djillali Liabes, BP89, Sidi Bel Abbès 22000, Algeria
[b] Laboratoire de Biochimie, INSERM, ERI 12, Centre Hospitalier Universitaire, Université de Picardie Jules Verne, Place Victor Pauchet, F-80000 Amiens, France
[c] Université d'Artois, Faculté Jean Perrin, Rue Jean Souvraz, SP18, 62307 Lens, France
[d] Laboratoire de Physique de la Matière Condensée, Université de Picardie Jules Verne, 33 rue St. Leu, 80039 Amiens, France

ARTICLE INFO

Article history:
Received 31 March 2010
Received in revised form 1 May 2010
Accepted 4 May 2010
Available online 12 May 2010

Keywords:
Thin films
Ferroelectric materials
Spray pyrolysis

ABSTRACT

Lithium metavanadate thin films were successfully deposited on glass substrates by spray pyrolysis technique at substrate temperature of 250 °C. 0.2 M spraying solution was prepared by mixing appropriate volumes of LiCl and VCl_3 solutions. Structural, vibrational and optical properties of deposited film are discussed. X-ray diffraction and micro-Raman spectroscopy have revealed that $LiVO_3$ with monoclinic symmetry was obtained. Optical properties of thin film were studied from transmission measurement in the range UV–Visible.

1. Introduction

Li–V–O system has been widely studied due to its applications in rechargeable lithium batteries, solid fuel cells or electrochromic display devices [1–4]. Orthovanadates of the type $M_3(VO_4)_2$ (M: Ca, Sr, Ba) have excellent luminescence properties which are enhanced when doped with suitable rare-earth element, and find application as laser host materials [5]. Metavanadate of the type MVO_3 (M: Li, Na, K, Rb, Cs) undergoes a ferroelectric (space group $C_C(C_s^4)$) to paraelectric (C_2/c) irreversible phase transition as function of temperature [6,7]. This transition is associated with very slight structural changes due to reorientations of the displacement ellipsoids of the lithium atoms [7].

$LiVO_3$ powdered or crystal samples were prepared by direct solid state reaction between stoichiometric proportions of Li_2CO_3 and V_2O_5 [7–9]. Coexistence of $LiVO_3$ and other phases such as Li_3VO_4 and $Li_xV_2O_5$ has been observed in lithium oxide vanadium powders prepared by the reaction of aqueous H_2O_2 solution with lithium and vanadium alkoxides, LiO-*n*-C_3H_7 and VO(O-i-C_3H_7)$_3$ [10]. Excessive starting Li/V molar ratio lead to the formation of $LiVO_3$, this result has been observed in the synthesis of $Li_{1+x}V_3O_8$ by sol–gel route at low temperature [11]. It has to be noticed that not having find studies concerning $LiVO_3$ thin films.

The aim of this work is to investigate X-ray diffraction, scanning electron microscopy, Raman and UV–Visible spectroscopy of $LiVO_3$ thin film prepared, in the first time, by spray pyrolysis technique.

2. Experimental

$LiVO_3$ thin films were obtained on glass substrates by spray pyrolysis technique. The spray solution 0.2 M, was prepared by mixing appropriate volumes of VCl_3 and LiCl solutions (80% LiCl + 20% VCl_3), bidistilled water was used as solvent. The substrate temperature was fixed at 250 °C and controlled through a thermocouple (Chrome–Nickel). Compressed air of pressure 2 bars has been used as a carrier gas, the solution flow is 5 cm^3/min and spray nozzle to heating plaque distance of 27 cm. The color of as-prepared films not having undergone treatment is light blue.

Structural characterization has been carried out at room temperature in the $\theta - 2\theta$ scan mode using a Rigaku Miniflex diffractometer (CuK_α radiation, λ = 1.5405 Å). Morphology of as-deposited thin film was observed using a Jeol JSM 5800 scanning electron microscope.

Raman spectroscopy measurements were performed at room temperature in a backscattering microconfiguration using the 514.5 nm line from an Ar-ion laser focused on the surface as a spot of 1 μm in diameter and with a power density of ~3 mW/cm^2. The scattered light was analyzed with a Jobin Yvon T64000 spectrometer, equipped with a liquid nitrogen cooled CCD detector. The spectrometer provided a wave number resolution better than 3 cm^{-1}.

Optical measurement of the transmittance was carried out in the wavelength range (200–900 nm) using a UV-Visible JASCO type V-570 double beam spectrophotometer.

3. Results and discussion

3.1. Structural properties

X-ray diffraction pattern of spray pyrolysed thin film is given in Fig. 1. The pattern exhibits several peaks in different directions indicating the polycrystalline nature of thin film. A good agreement

* Corresponding author. Fax: +213 48 54 41 00.
E-mail address: bouzidi_attou@yahoo.fr (A. Bouzidi).

0925-8388/$ – see front matter © 2010 Elsevier B.V. All rights reserved.
doi:10.1016/j.jallcom.2010.05.030

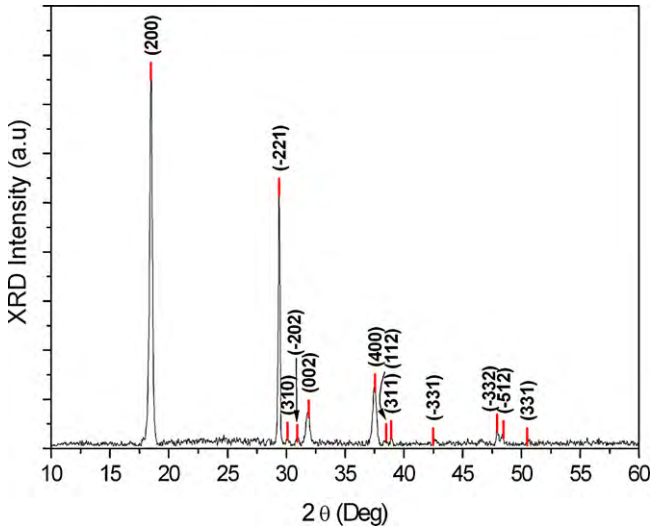

Fig. 1. X-ray diffraction pattern of spray pyrolysed $LiVO_3$.

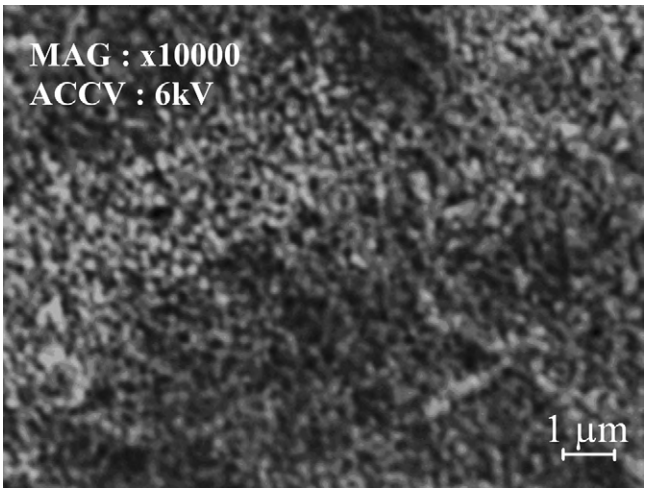

Fig. 2. SEM micrograph of spray pyrolysed $LiVO_3$ thin film.

is observed between the inter-reticular distances of obtained sample and those of ICCD card no. 73-1030 corresponding to the $LiVO_3$ with monoclinic symmetry. Only the polycrystalline phase of $LiVO_3$ was identified and no impurity was detected.

The peaks are indexed in comparing our experimental data (measured inter-reticular distances d_m and their diffracted intensities I_m) with the ICCD X-ray powder data file.

For monoclinic system, the inter-reticular distances d_{hkl} are evaluated by the following relation:

$$d_{h\,kl} = \frac{\sin\beta}{\sqrt{(h^2/a^2) + (l^2/c^2) + ((k^2\,\sin^2\beta)/b^2) - ((2hl\,\cos\beta)/(ac))}} \quad (1)$$

with $a \neq b \neq c$, $\alpha = \gamma = \pi/2$ and $\beta > \pi/2$.

In this relation (h, k, l) are miller indices of reflector plans appearing on the diffraction spectra and d_{hkl} their inter-reticular distances. Lattice parameters were refined with the CELREF program [12], the obtained values are summarized in Table 1. A very weak expansion of $LiVO_3$ lattice is observed and can be explained by the deposition conditions.

For the estimation of crystallite size the Sherrer formula is used [13]:

$$G = \frac{k\lambda}{D\,\cos(\theta)} \quad (2)$$

where k is the shape factor with value in the neighborhood of 1. D is defined as the full width at half maximum of more intense diffraction peak, λ is the Cuk_α wavelength and θ is the Bragg angle; the grain size is about 41 nm.

The surface morphology of the as-deposited film was studied using SEM and is shown in Fig. 2. It can be learned that, grains with regular shape and narrow lateral size compose the film, a low roughness of the surface is observed. The investigation of surface morphology was achieved without the treatment of the films.

Table 1
Lattice parameters obtained and comparison with literature data.

	a (Å)	b (Å)	c (Å)	β (°)	V (Å^3)
This work	10.22	8.27	5.95	110.91	470.51
ICCD card no. 73-1030	10.18	8.41	5.87	110.83	469.95
[7]	10.16	8.41	5.88	110.50	471.23

3.2. Raman micro-spectroscopy

The crystal structure of $LiVO_3$ has been determined for the first time by Shannon and Calvo by X-ray single crystal diffraction and has been described as monoclinic structure with space group $C_2/C(C_{2h}^6)$ in which bands of LiO_6 octahedra are linked by chains of VO_4 tetrahedra parallel to the c-axis [7,9].

According to C_{2h} factor group ($k = 0$) the crystal modes can be classified as follows:

$$\Gamma_{\text{opt}} = 22A_g + 20B_g + 20A_u + 22B_u \quad (3)$$

All the g modes are Raman active and u modes are Infrared active. Therefore 42 vibration modes are possible in the Raman spectroscopy of $LiVO_3$ [14].

Raman spectrum, in the range 100–1100 cm^{-1} is shown in Fig. 3. The spectrum clearly resembles that of $LiVO_3$, given in the literature [15]. All the observed Raman bands are listed in Table 2 and assigned in comparing with observed modes of $LiVO_3$ [14,15], a very good agreement is observed between our result and those of literature. In the high frequency region, the Raman bands are assigned to VO_2 stretching vibrations. The mean V–O distance of 1.65 Å for two exterior oxygen atoms is much shorter than of 1.808 Å for

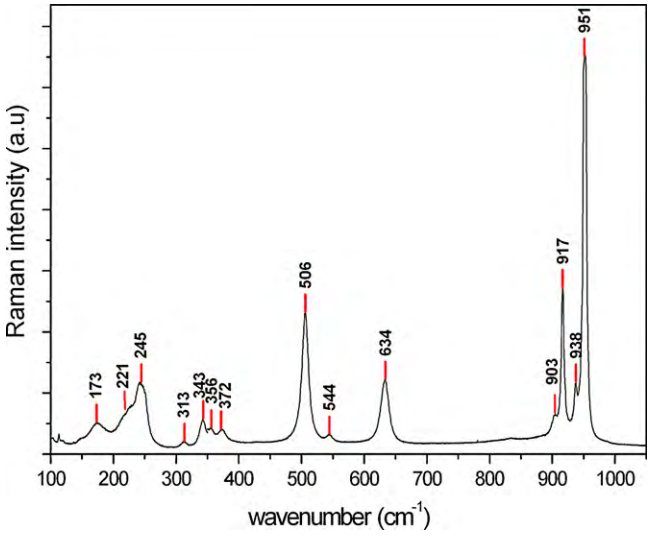

Fig. 3. Raman spectrum in the frequency range 1100–100 cm^{-1} of lithium metavanadate.

Table 2
Experimental frequencies (cm^{-1}) and assignment of the Raman active modes.

This work	Assignment [14, 15]	[15]	[14]
951 (vs)	$\nu_s(VO_2)$, (exterior)	952	954
938 (w)		939	
917 (s)		912	
903 (sh)	$\nu_s(VO_2)$, (backbone)	902	902.4
			820.6
		838	
			648.9
634 (m)	ν_a(VOV)	640	
			559.9
544 (w)	Mixed δ(VOV), $\nu(VO_2)$	540	
506 (s)	ν_s(VOV)	500	
372 (w)	δ(VO_2)	379	388.5
356 (w)		359	352.4
343 (w)		339	
		328	326
313 (vw)			
		265	267.3
244 (m)	ρ_r, ρ_t, ρ_w, Chain deformations	242	231.3
221(sh)	δ(VOV)	212	214.3
173 (m)	Lattice mode	185	160

s: strong, m: medium, w: weak, v: very, sh: shoulder, ρ_r, ρ_t, ρ_w: rock, wag, twist motions, δ: bending vibration, ν_s: symmetric stretching vibration, ν_a: asymmetric stretching vibration.

two backbone oxygen atoms [9]. Therefore the very intense Raman band observed at 951 cm^{-1} is assigned to VO_2 vibration involving the exterior oxygen atoms with V–O distance of 1.65 Å, and the band at 912 cm^{-1} to that involving the backbone oxygen atoms with V–O distance of 1.808 Å. While those in 500–650 cm^{-1} region, are assigned to the VOV vibrations, δVO_2 modes are observed in the 300 cm^{-1} region. The medium band observed at 244 cm^{-1} is related to the rock, wag, twist or deformation motions of the V–O chains and shoulder at about 213 cm^{-1} (lorentzian fitted value), is assigned to bending vibrations δVOV modes. Below 200 cm^{-1}, the Raman bands are assigned to lattice modes.

3.3. Optical characterization

Optical transmission for lithium metavanadate film measured in the range 300–900 nm is shown in Fig. 4a. The film presents absorption edge towards 300 nm and a maximum which reaches 58%. The optical absorption coefficient was evaluated by the approximate relation:

$$\alpha = \frac{1}{d}\ \mathrm{Ln}\ \frac{1}{T} \tag{4}$$

where T represents the transmission coefficient and d its thickness estimated towards 200 nm. The variation of absorption coefficient, as a function photon energy is presented in Fig. 4b (curve inserted). The values of α not exceed 8×10^4 cm^{-1}, this result can be explained by the influence of roughness or crystallization of the film.

The inter-band absorption theory shows that the absorption coefficient near the threshold versus incident energy is given by

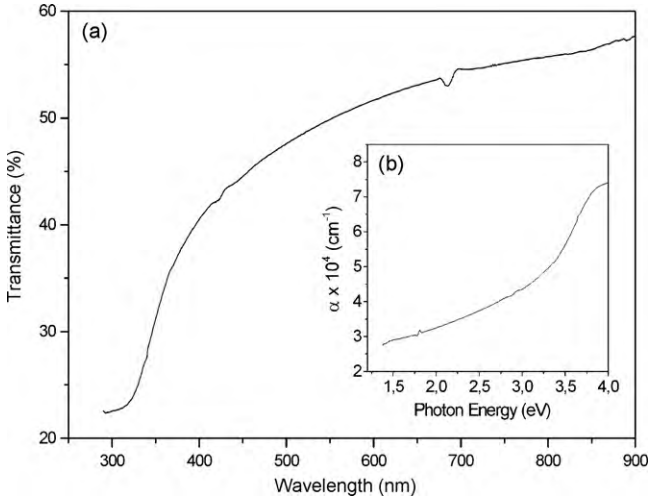

Fig. 4. (a) Transmission spectrum of $LiVO_3$ thin film and (b) (insert curve) absorption coefficient of $LiVO_3$.

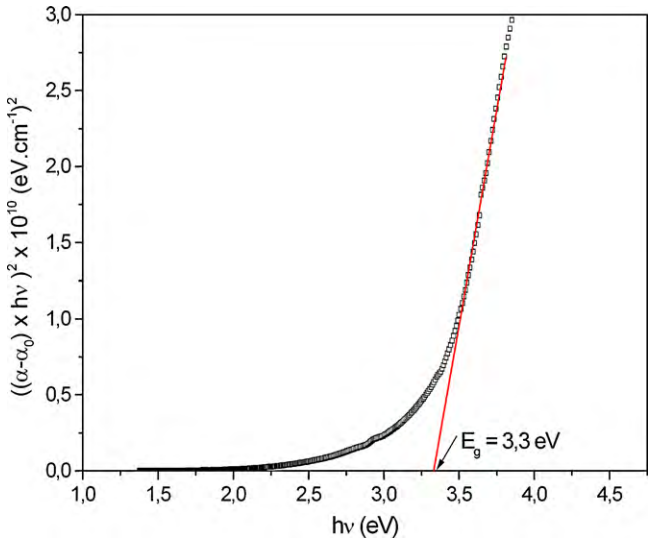

Fig. 5. $((\alpha - \alpha_0)h\nu)^2$ versus photon energy plot of $LiVO_3$ thin film.

the following relation [16]:

$$(\alpha h\nu) = A_n(h\nu - E_g)^n \tag{5}$$

where A_n is the probability parameter for the transition and E_g the optical gap energy.

For allowed direct transitions the coefficient n is equal to 1/2 and for indirect allowed transitions $n = 2$.

$((\alpha - \alpha_0)h\nu)^{1/2}$ do not present a linear character which suggests that $LiVO_3$ thin films prepared by spray pyrolysis technique have a direct gap. The variation of $((\alpha - \alpha_0)h\nu)^2$ is shown in Fig. 5, where α_0 characterizes the residual absorption. This curve presents a linear character which suggests that $LiVO_3$ thin films prepared by spray pyrolysis have a direct gap, the E_g value about 3.3 eV is estimated by extrapolation of linear part of $((\alpha - \alpha_0)h\nu)^2$ curve to the energy axis.

4. Conclusions

$LiVO_3$ thin films were prepared in the first time by spray pyrolysis technique. The structural results reveal that the prepared film exhibits a polycrystalline monoclinic structure. The value of average crystalline size is about 41 nm. Raman spectrum is well resolved

and all the Raman frequencies observed, correspond to $LiVO_3$ and confirm the XRD results. The optical band gap has been found to be 3.3 eV and corresponds to direct allowed transition.

References

[1] S. Prakash, W.E. Mustain, P.A. Kohl, J. Power Sources 189 (2009) 1184–1189.
[2] A. Hammou, A. Hammouche, Electrochim. Acta 33 (1988) 1719–1720.
[3] F. Wu, L. Wang, C. Wu, Y. Bai, Electrochem. Acta 54 (2009) 4613–4619.
[4] Y. Wang, G. Cao, Electrochem. Acta 51 (2006) 4865–4872.
[5] L.D. Morkle, A. Pinto, H.R. Verdon, B. McIntosh, Appl. Phys. Lett. 61 (1992) 2386–2388.
[6] S. Seetharama, H.L. Bhat, P.S. Narayanan, J. Raman Spectrosc. 14 (1983) 401–405.
[7] Ch. Muller, J.-C. Valmalette, J.L. Soubeyroux, F. Bouree, J.R. Gavarri, J. Solid State Chem. 156 (2001) 379–389.
[8] R.S. Feigelson, G.W. Martin, B.C. Johnson, J. Cryst. Growth 13 (1972) 686–692.
[9] R.D. Shannon, C. Calvo, Can. J. Chem. 51 (1973) 265–273.
[10] Mika Eguchi, Kiyoshi Ozawa, Electrochim. Acta 52 (2007) 2657–2660.
[11] Z.J. Wu, X.B. Zhao, J. Tu, G.S. Cao, J.P. Tu, T.J. Zhu, J. Alloys Compd. 403 (2005) 345–348.
[12] J. Laugier, B. Bochu, Cell parameters refinement program CELREF V3, http://www.inpg.fr/LMGP, 2003.
[13] L. Alexander, H.P. Klug, J. Appl. Phys. 21 (1950) 137–142.
[14] S.H. Tang, Z.X. Shen, C.W. Ong, M.H. Kuok, J. Mol. Struct. 354 (1995) 29–35.
[15] A. Grzechnik, P.F. McMillan, J. Phys. Chem. Solids 56 (1995) 159–164.
[16] P. Kereev, La Physique des Semiconducteurs, Mir, Moscow, 1975.